# FDTD Stability: Critical Time Increment

*Lukáš PAUK*[1], *Zbyněk ŠKVOR*[1]

[1] Dept. of Electromagnetic Field, Czech Technical University, Technická 2, 166 27 Praha, Czech Republic

paukl@fel.cvut.cz, skvor@fel.cvut.cz

**Abstract.** *A new approach suitable for determination of the maximal stable time increment for the Finite-Difference Time-Domain (FDTD) algorithm in common curvilinear coordinates, for general mesh shapes and certain types of boundaries is presented. The maximal time increment corresponds to a characteristic value of a Helmholz equation that is solved by a finite-difference (FD) method. If this method uses exactly the same discretization as the given FDTD method (same mesh, boundary conditions, order of precision etc.), the maximal stable time increment is obtained from the highest characteristic value. The FD system is solved by an iterative method, which uses only slightly altered original FDTD formulae. The Courant condition yields a stable time increment, but in certain cases the maximum increment is slightly greater* [2].

## Keywords

FDTD, stability, critical time increment, critical time step.

## 1. Introduction

Solution of Maxwell's equations in time domain is becoming increasingly important as a tool for microwave component analysis. The precision of electromagnetic field modeling is a complex question. One major factor that has a considerable influence on the precision is the time increment ($\Delta t$) of the FDTD algorithm. An optimal value of $\Delta t$ exists, resulting in the fastest and most precise computation. The other reason for setting this constant properly is that even a small excess over its optimal value would result in instability of the algorithm. There is a condition for $\Delta t$ called Courant [1], valid only for rectangular coordinates and an infinitely large mesh. A new approach has been used, applicable under more general conditions (mesh shapes, boundary conditions, general curvilinear coordinates (GCC)). In [7], [8] considerations on FDTD in GCC are presented, but conclusions are achieved only for GCC without curvature.

## 2. Theory

In order to describe the principle of the method, let us consider an example of FDTD in 2 dimensions only:

$$H_z^{n+\frac{1}{2}} = a_M H_z^{n-\frac{1}{2}} - b_M \operatorname{curl}_z\left(E_x^n, E_y^n\right) \qquad (1h)$$

$$E_x^{n+1} = a_E E_x^n + b_E \operatorname{curl}_x\left(H_z^{n+\frac{1}{2}}\right) \qquad (1e)$$

$$E_y^{n+1} = a_E E_y^n + b_E \operatorname{curl}_y\left(H_z^{n+\frac{1}{2}}\right) \qquad (1e')$$

where:

$$a_M = e^{-\frac{\sigma_M}{\mu}\Delta t} \quad , \quad b_M = \frac{1}{\sigma_M}\left(1 - a_M\right) \qquad (2h)$$

$$a_E = e^{-\frac{\sigma_E}{\varepsilon}\Delta t} \quad , \quad b_E = \frac{1}{\sigma_E}\left(1 - a_E\right) \qquad (2e)$$

These equations require comments:

- Time position of the field samples is marked by the upper suffix; $n$ is integral ( $n \in Z$ ).
- Space differences are not written in full, since the space scheme can be arbitrary. The space scheme is in fact an approximation (discretization) of the continuous *curl* vector operator and in (1) "*curl*" is only a placeholder for the particular discretization, valid for a particular coordinate system.
- It is marked explicitly what component of *curl* approximation is computed (lower suffix) and what it is computed from: e.g. in (1h) the $H_z$ component is updated using the $z$ component of *curl*, which is computed using both $E_x^n$ and $E_y^n$.
- For sake of simplicity, only a certain field mode is considered: field components remain constant in the direction of $z$ axis.
- The time scheme of (1) together with the constants (2) is applicable for media with significant losses [1]. Medium properties are described by $\sigma_E$, $\sigma_M$, $\varepsilon$ and $\mu$.

### 2.1 Time Dependence Cancellation, Formulation of Stability

In order to get frequency-domain formulae, let us substitute the following time dependence into (1).

$$E^n = E e^{j\varphi n} \quad , \quad H^{n+\frac{1}{2}} = H e^{j\varphi\left(n+\frac{1}{2}\right)} \qquad (3e,3h)$$

The field samples at the left-hand sides of (3), which depend on all the coordinates (the suffixes indicate position in time), are expressed as product of complex functions $E$

and $H$, which depend only on position in space, and time-dependent functions. Further, $j$ is the imaginary unit and $\varphi$ corresponds to angular frequency. Similar procedure can be found in [1].

The formulae follow:

$$\left(e^{+j\frac{1}{2}\varphi} - a_M e^{-j\frac{1}{2}\varphi}\right)\frac{1}{b_M} H_z = -\mathrm{curl}_z\left(E_x, E_y\right) \tag{4h}$$

$$\left(e^{+j\frac{1}{2}\varphi} - a_E e^{-j\frac{1}{2}\varphi}\right)\frac{1}{b_E} E_x = +\mathrm{curl}_x\left(H_z\right) \tag{4e}$$

$$\left(e^{+j\frac{1}{2}\varphi} - a_E e^{-j\frac{1}{2}\varphi}\right)\frac{1}{b_E} E_y = +\mathrm{curl}_y\left(H_z\right) \tag{4e'}$$

The formulae (4) present a set of equations for the unknown $\varphi$. The FDTD algorithm (1) is stable, only if the following condition is met for all possible solutions of (4) for $\varphi$:

$$\mathrm{Im}\{\varphi\} \geq 0\,. \tag{5}$$

The solutions of (4) must be discussed with respect to $\Delta t$ ($\Delta t$ is hidden in the coefficients of (4)), which has to be as great as possible, but not violating the stability condition (5).

For the precise formulation of stability a supplementary condition must be specified. Without this condition one would derive that instability occurs, only if $\Delta t > \Delta t_c$, whereas it can be proved that $\Delta t \geq \Delta t_c$ is correct. Although this has no practical use, we found inevitable to mention it. We will only outline the reason of instability for $\Delta t = \Delta t_c$ and formulation of the supplementary condition:

The fact is that the algorithm can be instable even for $\mathrm{Im}\{\varphi\}=0$ (which is admitted by (5)), though the functions (3) themselves are bounded for $\mathrm{Im}\{\varphi\}=0$. Instability occurs for this special case ($\mathrm{Im}\{\varphi\}=0$), only if there are two solutions of (4) (field modes) with the values $\varphi$ equal to $\pi$ and $-\pi$. This special case should be excluded from the definition of stable conditions in the formulation of stability (by means of the supplementary condition). The reason of instability in this special case can be outlined only in short at this place: The resulting time behavior (3) of the two modes (with $\varphi$ equal to $\pi$ and $-\pi$) become linearly dependent (this phenomenon could not occur for continuous counterpart of (3)). Therefore if there are two modes with $\varphi$ approaching to $\pi$ and $-\pi$, then an attempt to express an initial field distribution of (1) by means of a linear combination of modes would result in the increasing absolute value of the coefficients of the two modes above all limits. The stability limit is characterized by presence of a mode with $\varphi = \pi$ (see next chapters) and this mode always has its counterpart with $\varphi = -\pi$ (consider (4)). Therefore exactly at the stability limit the algorithm is instable. At the end we can note that near the stability limit the coefficients of the two modes can be significantly greater than all other coefficients. In an experiment (1), oscillations of these two modes (the other modes appear only as noise) can be observed in the mesh. The two modes are distorted (see chapter 2.3) and their great amplitudes may influence the computer numeric. This can happen, however, only if $\Delta t$ is extremely close to $\Delta t_c$.

## 2.2 Lossless Case

First, let us consider lossless case ($\sigma_E = \sigma_M = 0$). The formulae (4) will have the following form; let us define a constant $k$, which is apparent from (6e').

$$\tfrac{2}{\Delta t}\sin\left(\tfrac{1}{2}\varphi\right) j\mu H_z = -\mathrm{curl}_z\left(E_x, E_y\right) \tag{6h}$$

$$\tfrac{2}{\Delta t}\sin\left(\tfrac{1}{2}\varphi\right) j\varepsilon E_x = +\mathrm{curl}_x\left(H_z\right) \tag{6e}$$

$$\underbrace{\tfrac{2}{\Delta t}\sin\left(\tfrac{1}{2}\varphi\right)}_{k} j\varepsilon E_y = +\mathrm{curl}_y\left(H_z\right) \tag{6e'}$$

A method described in the next chapter is used to obtain the values of $k$. For the calculations in this chapter it is necessary to know that: **i)** these values are real ($k \in R$), **ii)** there is a finite number of them, **iii)** for each $k$ there is also $-k$. Here it is to discuss only the relationship among $k$, $\varphi$ and $\Delta t$, which is defined in (6e'):

$$\tfrac{1}{2} k\Delta t = \sin\left(\tfrac{1}{2}\varphi\right). \tag{7}$$

It can be seen that the maximum value of $\Delta t$, for which (5) is true for all the possible values of $k$, is given by (7) when

$$\varphi = \pi \tag{8}$$

Further, the maximum value of $k$ ($k_m$) must be substituted:

$$\tfrac{1}{2} k_m \Delta t_c = 1 \tag{9}$$

## 2.3 Solution of the Finite-Difference (FD) Scheme for Helmholz Equation

The equation set (6), which is to be solved, is in fact a finite-difference (FD) scheme that can be used to solve a Helmholz equation numerically; the Helmholz equation can be obtained by elimination of $E$ from (6):

$$\underbrace{-\tfrac{1}{\mu}\mathrm{curl}_z\left[\tfrac{1}{\varepsilon}\mathrm{curl}_x\left(H_z\right), \tfrac{1}{\varepsilon}\mathrm{curl}_y\left(H_z\right)\right]}_{\Delta H_z} + k^2 H_z = 0 \tag{10}$$

This form (10) can be used to denote both the continuous Helmholz equation and its FD scheme. The latter can be obtained, if the particular discretization is substituted for *curl*. In this case the notation $\Delta$ would not stand for the continuous Laplace operator, but for its discrete equivalent.

The solutions of (10) are characteristic functions (called modes), corresponding to characteristic values $k$.

In [2] a method for solving a discrete system like (10) or (6) is presented. It makes use of the variable separation principle and therefore it can handle only certain boundary conditions. A more general iterative method [3] can be used:

The term $\Delta H_z$ is evaluated at all the mesh points and these values are used to compute $k$ by means of (10). Because (10) is not satisfied, different values $k$ will be obtained at every mesh point. Rayleigh's formula is used to produce an estimation of $k$. Then, this estimation together with the values $\Delta H_z$ is used to correct the distribution of $H$ using (10). The process is stopped if the change in $k$ is sufficiently small.

In order to obtain the correct $k$ (and hence $\Delta t_c$), the FD scheme (10) must be exactly the same as the space scheme of the FDTD method itself (i.e. the same spacing of corresponding samples, boundary conditions, order of precision, coordinate system). It is easy to fulfil this condition and moreover it is not necessary to eliminate $E$ components from (6) as it is suggested in (10). The desired values of $\Delta H_z$ can be easily obtained directly from (6) in two steps: First, $E$ is computed from $H$ using (6e,6e'). The values of $H$ computed back from $E$ using (6h) are the values of $(1/k^2)\Delta H_z$. It is simple to change the programmed FDTD (1) and obtain the FD form (6).

Following comments must be pointed out:

- The mesh can have arbitrary shape, but the simplest conditions at the boundaries (zero elements, $E$ or $H$) are assumed in the following text. (Correct results were obtained for certain more complicated conditions, but let us not discuss it in this paper).

- It holds that $k \in R$. One could think at first glance at (6) that it is necessary to use complex arithmetic, but it is not inevitable (consider e.g. the substitution $H = jH'$).

- A discrete mode with the maximal characteristic value $k_m$ exists (unlike the continuous case).

- The material properties $\varepsilon$ and $\mu$ in (10) (and thus also in (6)) need not be independent on space position (although in this case naming the equation Helmholz may not be justified). Convergence of the method was verified experimentally.

- The discrete mode with the maximal $k$ is distorted so much that it cannot be considered to be an approximation of a continuous mode any more (it is possible only for low $k$).

Iterations of this method require an initial space distribution of $H_z$. It shows that the corresponding mode of interest (the one with $k_m$) has the following property: all the samples neighboring in the directions of all the space coordinates have opposite sign. In order to obtain the mode of interest, the initial distribution has to respect this. In all the experiments the following distribution yielded the desired mode:

$$H_z\big|_{x=i\Delta x+x_0,\ y=j\Delta y+y_0} = (-1)^{i+j} \tag{11}$$

where $i,j$ are integer indices to the field of samples. The formula does not hold for the zero $H$ samples at the boundary (if there are any). The formula is valid for our 2-dimensional example, but it can be extended to 3 dimensions easily.

## 2.4 Lossy Case

It is necessary to solve and discuss the general formulae (4). Let us mark the coefficients of (4) as $k_E$, $k_M$, and adjust them:

$$\underbrace{\tfrac{1}{b_E}\left(e^{+\frac{j}{2}\varphi} - a_E e^{-\frac{j}{2}\varphi}\right)}_{jk_E} = j\sigma_E \frac{\sin\left(\frac{1}{2}\varphi - \frac{j}{2}\frac{\sigma_E}{\varepsilon}\Delta t\right)}{\sinh\left(\frac{1}{2}\frac{\sigma_E}{\varepsilon}\Delta t\right)} \tag{12e}$$

$$\underbrace{\tfrac{1}{b_M}\left(e^{+\frac{j}{2}\varphi} - a_M e^{-\frac{j}{2}\varphi}\right)}_{jk_M} = \cdots \tag{12h}$$

In the lossless case it was possible to obtain the FD scheme for the Helmholz equation in the form (10), thanks to the fact that $k$ (see (6e')) was constant. In this case, however, $k_E$ , $k_M$, may vary with space position (according to material properties), which would produce a FD scheme with variable and (moreover) non-linear coefficients. Despite these facts an experiment employing a modified method from the previous chapter was found to yield correct results. The only fault is that in this general case we were not able to prove the condition for the limit of stability, which, as experiments show, is given by (8), again.

We were able to prove this fact only for the case of constant material properties: In this case $k_E$ and $k_M$ are constant as well and a formula like (10) can be obtained (in (10), $\varepsilon$ and $\mu$ must be removed (set to 1) and $k_E k_M$ substituted for $k^2$). We will show certain steps of the proof only for the special case $\sigma_M/2\mu = \sigma_E/2\varepsilon = p$. The formula, corresponding to (7) in the lossless case, follows:

$$\frac{k^2}{\sigma_E \sigma_M}\sinh^2(p\Delta t) = \sin^2\left(\tfrac{1}{2}\varphi - jp\Delta t\right). \tag{13}$$

The left-hand side of (13) is linearly proportional to $k^2$, proportional to $\Delta t$ and is always real and non-negative. The right-hand side is real, if the argument of *sin* is real or if $\mathrm{Re}\{\varphi\} = \pi$. Until the left hand side is smaller than 1, its growth (due to greater $\Delta t$ or $k$) can be compensated by growth of $\mathrm{Re}\{\varphi\}$, provided that $\mathrm{Im}\{\tfrac{1}{2}\varphi\} = p\Delta t$. After that (when *sin* reaches its maximum in real domain) the compensation is accomplished either by increase or decrease of $\mathrm{Im}\{\varphi\}$ (two roots, each of which can spoil stability), while $\mathrm{Re}\{\varphi\}$ has to remain equal to $\pi$. Decreasing $\mathrm{Im}\{\varphi\}$ can become negative, which means instability.

The formula (13) could be used to determine $\Delta t_c$, if (8) and $k_m$ were substituted into it. We used a different method, capable to handle even the fully general case:

Let us write (4) for the stability limit (8), let us define the symbols $\varepsilon'$, $\mu'$ and let us introduce an artificial constant $k'$:

$$k'j\underbrace{\frac{1+a_M}{1-a_M}\sigma_M}_{\mu'}H_z = -curl_z\left(E_x, E_y\right) \tag{14h}$$

$$k'j\frac{1+a_E}{1-a_E}\sigma_E\, E_x = +curl_x\left(H_z\right) \tag{14e}$$

$$k'j\underbrace{\frac{1+a_E}{1-a_E}\sigma_E}_{\varepsilon'}E_y = +curl_y\left(H_z\right) \tag{14e'}$$

In order to get the correct $\Delta t_c$, $k'$ must be equal to 1. Introducing $k'$ results in a set that we are able to solve (the set has the form of (6) now). Direct solution is not possible because the coefficients of (14), i.e. $\varepsilon'$ and $\mu'$ are nonlinear functions of position and the unknown $\Delta t_c$. What we can do is to solve (14) for $k'$, use it ($k'$) for correction of $\Delta t_c$ and repeat the procedure, until $k'$ is close enough to 1. Prior to computing $k'$, the coefficients $\varepsilon'$ and $\mu'$ must be known, therefore an initial guess of $\Delta t_c$ is required.

After an ideal correction of $\Delta t_c$ the values of $\mu'$ (and similarly $\varepsilon'$) in every mesh cell should change $k'$-times. In such an ideal case it would be possible to set $k'$ to 1 as required and (14) would remain to be satisfied because such a correction would not change the set (14) in fact. We would arrive to the solution in one step. It could be done, however, only if the material properties were independent on space position or for certain dependence of $\mu'$ and $\varepsilon'$ on $\Delta t_c$ (consider lossless case). Otherwise it is not possible to achieve the ideal correction for all the mesh cells and more iterations are inevitable.

In the experiment the correction $\Delta t_c^{i+1} = \Delta t_c^i k'^i$ was used and the method showed to be convergent. We have not proved this, but the character of the dependence of $1/\mu'$ and $1/\varepsilon'$ on $\Delta t_c$ promise not to disturb the stability: The derivative of these functions is positive and does not increase as $\Delta t_c$ grows. Therefore if $\Delta t_c$ changes $k'$-times ($k'>0$), the change in $\mu'$ (or $\varepsilon'$) is smaller than $k'$-times or is exactly $k'$-times (if the material in the given space cell is lossless).

## 2.5 Compact Notation of FDTD Update Formulae

This chapter is added here not only in order to save space during description of the experiment. A very simple, yet exact and well-suited notation, which is especially convenient for theoretical derivations, will be presented. The compact form can be used for abbreviation of the FDTD formulae in rectangular [1] and cylindrical [4] coordinates and it yields the general form of the coefficients (2) [1]. FDTD in spherical coordinates, an algorithm of adequate complexity for our experiment, was not found in any literature and therefore it was constructed using this approach.

The compact scheme is a result of expressing Maxwell's equations **i)** for corresponding coordinate system, **ii)** in differential form, **iii)** as a sum of so-called self-adjoined terms:

$$\frac{1}{g}\frac{\partial}{\partial u}(fC) \tag{15}$$

where $C$ is a field component, $u$ stands for a coordinate ($x$, $y$, $z$ or $t$) and $g, f$ for a function.

It is always possible to write the equations this way, as we can make use of the *curl* operators written by means of the local length units $h_x$, $h_y$, $h_z$ (see e.g. [5]). An example, the first Maxwell's equation for one vector component, follows:

$$\underbrace{\frac{1}{h_y h_z}\left[\frac{\partial}{\partial y}\left(h_z H_z\right) - \frac{\partial}{\partial z}\left(h_y H_y\right)\right]}_{\mathrm{curl}_x H} = \underbrace{\frac{\varepsilon}{e^{\frac{\sigma}{\varepsilon}t}}\frac{\partial}{\partial t}\left(e^{\frac{\sigma}{\varepsilon}t}E_x\right)}_{\sigma E_x + \varepsilon\frac{\partial}{\partial t}E_x} \tag{16}$$

This equation holds for the coordinate $x$ of the coordinate system; – the other 2 equations can be obtained by cyclic interchange of indices $x$, $y$, $z$. The second Maxwell's equation is analogous.

The FDTD is defined by the discretization prescription (or approximation) of (15). Different prescriptions result in different algorithms with corresponding order of precision. The following prescription is considered here:

$$\frac{1}{g}\frac{\partial}{\partial u}(fC) \equiv \frac{1}{\frac{1}{\Delta u}\int_I g\, du}\cdot\frac{f^{+\frac{1}{2}}C^{+\frac{1}{2}} - f^{-\frac{1}{2}}C^{-\frac{1}{2}}}{\Delta u} \tag{17}$$

Explanation, further specifications of (17) and comments are required; let us suppose that we want to write the approximation (17) for the point $[t_0, x_0, y_0, z_0]$:

- The generic coordinate $u$ in (17) can stand for $x$, $y$, $z$, $t$.
- Difference of 2 neighboring field samples, $C^{-\frac{1}{2}}, C^{+\frac{1}{2}}$ is used. The samples are located $-½\Delta u$ and $+½\Delta u$ (respectively) in the direction $u$ from the point of approximation.
- The difference is weighted by corresponding values of $f$ – samples of $f$ are taken at the points of the samples $C^{-\frac{1}{2}}, C^{+\frac{1}{2}}$.
- The interval, along which the integral is computed, is an oriented abscissa from the point of $C^{-\frac{1}{2}}$ to $C^{+\frac{1}{2}}$ – all the coordinates except for $u$ are constant.
- It is necessary to respect the fact that the approximation is valid at $[t_0, x_0, y_0, z_0]$ (which is known as central-difference principle). Approximation of all the terms of Maxwell's equations has to be valid at the same point. This fact induces formation of the corresponding discretization mesh [6].

Let us give an example – discretization of the right-hand side of (16), which yields the general coefficients (2):

Let us rewrite (16), abbreviating its left-hand side as *curl* and expanding only the right-hand side according to (17). (The coordinate $u$ in the general formula (15) stand for $t$, $f$ for $e^{\frac{\sigma}{\varepsilon}t}$, $g$ for $\frac{1}{\varepsilon}e^{\frac{\sigma}{\varepsilon}t}$ and $C$ for $E_x$):

$$\operatorname{curl}_x^n H = \frac{e^{\frac{\sigma}{\varepsilon}\left(t_n+\frac{1}{2}\Delta t\right)} E_x^{n+\frac{1}{2}} - e^{\frac{\sigma}{\varepsilon}\left(t_n-\frac{1}{2}\Delta t\right)} E_x^{n-\frac{1}{2}}}{\Delta t \cdot \frac{1}{\Delta t}\int_{t_n-\frac{1}{2}\Delta t}^{t_n+\frac{1}{2}\Delta t} \frac{1}{\varepsilon} e^{\frac{\sigma}{\varepsilon}t}\, dt}. \tag{18}$$

Upper suffix denotes time position of the sample: $E_x^n$ is the sample of $E_x$ at $t_n=n\Delta t$. The approximation is valid for time instant $n$, therefore the same must be true for the remaining terms of the Maxwell's equation (which are "hidden" in *curl*) – this is marked by the suffix $n$ at *curl*. The space coordinates remain constant, therefore we avoided to write 3 more space indices in (18).

If the formula (18) were explicit for $E_x^{n+\frac{1}{2}}$, we would obtain an expression only slightly different from (1e). In order to obtain (1e) exactly, one must make one more substitution into (18). It is self-evident, that field samples in an equation set (like (1), e.g.) must match. The equation (18), as is, would match (1h,1e'), only if $(n+\frac{1}{2}) \in Z$. The transition $n \to n+\frac{1}{2}$ makes possible to write $n \in Z$, as it is assumed for (1).

# 3. Experiments

The method was tested in many experiments. For the experiments in rectangular, cylindrical and spherical coordinates described in [2] the same results were obtained. Both the methods yielded slightly different results compared to the Courant condition [1] (rectangular coordinates). Despite this fact the results are correct. Experiment verified that the Courant condition yields a stable $\Delta t$ but in certain cases $\Delta t_c$ is slightly greater [2].

A detailed and unique description of an experiment with FDTD in spherical coordinates follows.

## 3.1 FDTD Update Formulae

As an example, we will outline derivation of the update formula for $E_r$.

The local length units for the spherical coordinates $(r,\vartheta,\varphi)$ are $1, r, r\sin\vartheta$ respectively, hence the left-hand side of (16) follows:

$$\underbrace{\frac{1}{r\sin\vartheta}\frac{\partial}{\partial\vartheta}\left(H_\varphi \sin\vartheta\right) - \frac{1}{r\sin\vartheta}\frac{\partial}{\partial\varphi}H_\vartheta}_{\operatorname{curl}_r H} \tag{19}$$

The discretization of (19) can be readily written:

$$\operatorname{curl}_r^{n,i,j,k} H = \frac{1}{R^i}\frac{S^{j+\frac{1}{2}}H_\varphi^{n,i,j+\frac{1}{2},k} - S^{j-\frac{1}{2}}H_\varphi^{n,i,j-\frac{1}{2},k}}{\Delta\vartheta \cdot \Phi^j} - \frac{1}{R^i S^j}\frac{H_\vartheta^{n,i,j,k+\frac{1}{2}} - H_\vartheta^{n,i,j,k-\frac{1}{2}}}{\Delta\varphi} \tag{20}$$

Explanation:

- The upper indices $n$, $i$, $j$, $k$ indicate position of samples: e.g. $H^{n,i,j,k}$ is the value at the point $\left[t_n, r_i, \vartheta_j, \varphi_k\right]$, where $t_n=n\Delta t$, $r_i=i\Delta r$,...
- $R$ and $S$ stand for samples of the functions $r$ and $\sin\vartheta$ (respectively) at the points given by the suffixes. (Those suffixes, on which the given function does not depend, are omitted.)

For the second term in (19) the function '$r\sin\vartheta$' is constant in $\varphi$, therefore the result of the corresponding average integral in (17) is simply $R^i S^j$. In the first term only the function $r$ is constant in $\vartheta$, therefore the result is $R^i\Phi^j$, where $\Phi^j$ is the average of '$\sin\vartheta$' on the corresponding abscissa, i.e.:

$$\Phi^j = \frac{1}{\Delta\vartheta}\int_{\vartheta_j-\frac{1}{2}\Delta\vartheta}^{\vartheta_j+\frac{1}{2}\Delta\vartheta} \sin\vartheta\, d\vartheta. \tag{21}$$

At this place we made a simplification in the formulae of the experiment. In all cases the average of '$\sin\vartheta$' was approximated by the value of '$\sin\vartheta$' at the center of the abscissa, i.e. $\Phi^j \equiv S^j$ simply.

In order to get the update formula for $E_r$, (20) and (18) must be combined. Prior to that, $x \equiv r$ must be substituted into (18) and (18) must be augmented by the left-out space indices.

## 3.2 Other Specifications of the Experiment

Simple boundary condition was used: electric walls placed directly to the tangential components of $E$. The shape of FDTD mesh was a "cube" in spherical coordinates with the walls at $R_{1;2}$=10;15, $\Theta_{1;2}$=1;1.5, $\Phi_{1;2}$=0;1. The number of cells in the corresponding directions was 15;10;5. In some cases this region was made more complex: In the sub-region that spans 3 cells in $r$ direction from the wall at $R_1$, all the cells from the wall at $\Theta_1$ were cut off by the electric wall to the depth of 3 cells and similarly from the wall $\Phi_1$ to the depth 2. The medium was considered lossless, with $\varepsilon=\mu=1$, except (in some cases) for the following belt: The $E$ components at $r \in \langle R_1+3\Delta r, R_1+5\Delta r\rangle$ were updated using the constants $a_E$, $b_E$ (see (2)) corresponding to $\sigma_E$=1. Altogether $2\times 2$ cases were investigated: a cube or a complex region with or without losses.

## 3.3 Results

In the case of cube with losses $\Delta t_c$=0.289012 and it was determined by the mode $H_r$=0 (the time increment obtained from the mode $E_r$=0 was slightly higher: 0.289068). (The indicated precision was obtained in cca 300 iterations without relaxation.) In the case of cube without losses $\Delta t_c$=0.2884806. In the case of complex region with and without losses $\Delta t_c$=0.290303 and 0.289759 respectively.

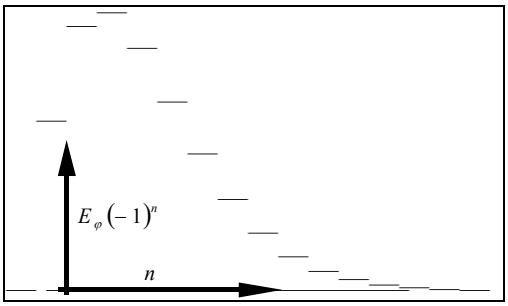


**Fig. 1.** Discretized field strength of the critical mode plotted against mesh index $n$, along structure radius.

Fig.1 demonstrates a typical waveform of the mode that determines instability. It is a waveform of the component $E_\varphi$ along the $r$ coordinate (with fixed $\vartheta$ and $\varphi$). The waveform forms an alternating series: the product of adjacent samples is non-positive, but in Fig.1 the rectified waveform was plotted. The zero samples at the boundaries $R_1$,$R_2$ are included.

### 3.4 Remarks to 3 Dimensions

In an equation set for 3 dimensions no elimination like (10) is possible in general. Despite that, fortunately, the experiment yielded correct value $\Delta t_c$.

During the iterations described in chapter (2.3) the characteristic value is estimated from samples of magnetic field $H$. $H$ field is used because in (6) there is only one component of this field. In general case there will be all 3 components for both $E$ and $H$. In our 3-dimensional experiment only the $r$ components were used for the purpose. Depending on whether it was $E_r$ or $H_r$, the experiment yielded 2 characteristic values. The critical time increment was determined by the greater one.

### 3.5 FDTD in Rectangular Coordinates with Inhomogeneous Material

We employed an algorithm in rectangular coordinates in two dimensions and investigated influence of permittivity distribution on the critical time increment $\Delta t_c$.

The shape of the mesh was a rectangle, whose boundaries passed only through the samples of tangential components of electric field. At the boundaries the components were set zero. Material was lossless, with $\mu$=1. In some cases the initially uniform permittivity distribution ($\varepsilon_1$=8) was replaced by lower permittivity ($\varepsilon_2$=2) in certain mesh cells.

According to Courant condition [1] the critical time increment for the initial distribution $\varepsilon_1$ is $\Delta t_{c1}$=2, if the permittivity in the whole region is $\varepsilon_2$, $\Delta t_c$ decreases to $\Delta t_{c2}$=1. As a result of the boundary conditions in the experiment, the exact $\Delta t_c$ was negligibly greater [2]. (Let us define that relative change of $\Delta t$ is negligible or practically zero, if it has negligible influence on speed of computations – let us say, if it is <0.5%).

The experiment yielded some interesting conclusions:

If cells with $\varepsilon_1$ are being replaced by $\varepsilon_2$, the increment $\Delta t_c$ drops rapidly to $\Delta t_{c2}$, provided that a compact region of $\varepsilon_2$ is being formed. If there is at least one region of $\varepsilon_2$ that is at least 10x10 cells large, $\Delta t_c$ is practically given by $\Delta t_{c2}$ (Courant condition). Dependence on the mesh dimensions ($N_x$,$N_y$) and position of the region in the mesh is negligible.

If the $\varepsilon_2$ cells are scattered, on the other hand, $\Delta t_c$ can be significantly greater than $\Delta t_{c2}$: we scattered as many as 30x30 cells into a 100x100 mesh, so that there were no adjacent $\varepsilon_2$ cells and the resulting $\Delta t_c$ was greater by cca 38%.

Perhaps there is a practical application, for which the method can yield a more efficient and stable $\Delta t$.

### 3.6 Verification of Results

The obtained critical time increment $\Delta t_c$ was verified experimentally by means of the FDTD algorithm itself. In order to verify that our critical time increment holds, we made two experiments with $\Delta t$ slightly over (relative change cca $10^{-6}$) and then slightly under our predicted $\Delta t_c$. In all cases, exceeding predicted $\Delta t_c$ values caused instability while lower values proved to be stable.

To be on a safe side, we recomputed the field for long periods to be sure that no other mode does appear.

## 4. Conclusion

A versatile and easy-to-use method capable of precise determination of the critical time increment for FDTD was presented. The results were verified experimentally for a FDTD in spherical coordinates for inhomogeneous medium and non-trivial mesh shapes. The authors assume this method to be new.

## Acknowledgements

This research and publication have been sponsored by the Czech Grant Agency, contracts no. 102/01/0571 and 102/01/0573, and by the Czech Ministry of Education in the frame of project MSM 210000015.

## References

[1] TAFLOVE, A. *Computational electrodynamics – the finite-difference time-domain method.* Artech House, Boston, London, 1995.

[2] PAUK, L., SKVOR, Z. Stability of FDTD in curvilinear coordinates. In*: EUROCON 2001.* Bratislava, IEEE, 2001, p. 314-317, vol. 2.

[3] DAVIES, J. B. , MUILWYK, A. Numerical solution of uniform hollow waveguides with boundaries of arbitrary shape. *Proc. IEE* (London), 1966, vol. 133, pp. 277-284.

[4] CHEN, Y., MITRA, R., HARMS, P. Finite-difference time-domain algorithm for solving Maxwell's equations in rotationally symmetric geometries. *IEEE Trans. on MTT,* 1996, *v*ol. 44, no. 6.

[5] ANGOT, A. *Complements de mathematique a l'usage des ingenieurs de l'electrotechnique et des telecommunications*. MASSON et Cie (Editions de la Reuve d'Optique, Paris, 1952.

[6] YEE, K. S. Numerical solution of initial boundary value problems involving Maxwell's equations in isotropic media. *IEEE Trans. Antenna Propagat,*1966, vol. AP-14.

[7] NAVARO, E. A., WU, CH., CHUNG, P.,Y., JOHN L. Some considerations about the Finite Difference Time Domain Method in General Curvilinear Coordinates. *IEEE Microwave and Guided Wave Letters,* 1994, vol.4, no.12.

[8] XIAO, F., YABE, H. Numerical dispersion relation for FDTD method in general curvilinear coordinates. *IEEE Microwave and Guided Wave Letters,*1997, vol.7, no.2.

## About Authors...

**Lukáš PAUK** was born in 1975 (Čeladná, Frýdek-Místek). In 1999 he received Ing. (M.Sc.) degree from the Czech Technical University in Prague, Czech Republic. Nowadays he continues studying as a postgradual student.

**Zbyněk ŠKVOR** graduated from CTU in Prague, 1985. He is with the Department of Electromagnetic Field, CTU Prague. His field of interest includes numerical electromagnetics, CAD for radio-frequency and microwave circuits and microwave measurements.